Biorheology 47 (2010) 1–14
DOI 10.3233/BIR-2010-0559
IOS Press

Stress relaxation and recovery in tendon and ligament: Experiment and modeling

Sarah E. Duenwald [a], Ray Vanderby Jr. [a,b] and Roderic S. Lakes [a,c,*]
[a] *Department of Biomedical Engineering, University of Wisconsin–Madison, Madison, WI, USA*
[b] *Department of Orthopedics and Rehabilitation, University of Wisconsin–Madison, Madison, WI, USA*
[c] *Department of Engineering Physics, University of Wisconsin–Madison, Madison, WI, USA*

Received 30 July 2009
Accepted in revised form 4 February 2010

Abstract. Accurate joint models require the ability to predict soft tissue behavior. This study evaluates the ability of constitutive equations to predict the nonlinear and viscoelastic behavior of tendon and ligament during stress relaxation testing in a porcine model. Three constitutive equations are compared in their ability to model relaxation, recovery and reloading of tissues. Quasi-linear viscoelasticity (QLV) can fit a single stress relaxation curve, but fails to account for the strain-dependence in relaxation. Nonlinear superposition can fit the single relaxation curve and will account for the strain-dependent relaxation behavior, but fails to accurately predict recovery behavior. Schapery's nonlinear viscoelastic model successfully fits a single relaxation curve, accounts for strain-dependent relaxation behavior, and accurately predicts recovery and reloading behavior. Comparing Schapery's model to QLV and nonlinear superposition, Schapery's method was uniquely capable of fitting the different nonlinearities that arise in stress relaxation curves from different tissues, e.g. the porcine digital flexor tendon and the porcine medial collateral ligament (MCL), as well as predicting subsequent recovery and relaxation curves after initial loads.

Keywords: Viscoelasticity, quasi-linear viscoelasticity, nonlinear superposition, tendon, ligament

1. Introduction

Many investigators have developed 3-D models of diarthrodial joints such as the knee or ankle. In order to create an accurate model, it is important to use correct anatomy of bones and soft tissues, and to accurately simulate behavior of such tissues. Not only is it important to be able to predict behavior during an initial loading, but also during unloading and reloading, since many functional loads are cyclic. Multiple constitutive equations, including quasi-linear viscoelasticity [1,10,11,13], nonlinear superposition [17,20], visco-hyperelasticity [2] and Schapery's nonlinear viscoelastic model [20,24,25] have been used to successfully fit a single stress relaxation or single creep curve of biological tissue well. However, soft tissues usually undergo repeated cycles of loading and unloading *in vivo*. Therefore, a robust constitutive equation should be able to model the behavior of the tissue under more complex loading histories.

Tendon and ligament are often considered interchangeable in surgical applications and treated as identical tissues, but they have been shown to exhibit different viscoelastic behavior. In the case of ligament,

* Address for correspondence: Dr. Roderic S. Lakes, Department of Engineering Physics, University of Wisconsin–Madison, 1500 Engineering Drive, 541, Madison, WI 53706-1687, USA. E-mail: lakes@engr.wisc.edu.

the rate of stress relaxation decreases with increasing strain [3,15,21]. In contrast, the rate of stress relaxation in tendon has been shown to increase with increasing strain [4,7,8,19,26]. An ideal model would be flexible enough to adjust to either trend in stress relaxation rate in order to best predict the viscoelastic behavior of a given material.

In this study, we examine the ability of constitutive equations in the literature to model behavior of tendon and ligament tissues. These constitutive equations differ as follows. Linear viscoelasticity entails a relaxation modulus independent of strain and a creep compliance independent of stress. Soft tissue under physiological deformation exhibits sufficient nonlinearity that a linear viscoelastic model is inadequate. QLV allows for some nonlinearity of a particular type. Specifically, the relaxation modulus can depend on strain, but the shape (functional form) of all relaxation curves is identical. Recovery following relaxation must follow the same time dependence as relaxation in QLV. Nonlinear superposition allows the relaxation modulus to depend on strain; the shape of the relaxation modulus vs. time curves can also depend on strain. Similarly, the shape of creep curves can depend on stress. A single experimental relaxation or creep curve is insufficient to distinguish among linear viscoelasticity, QLV or nonlinear superposition. If one supplements such a relaxation with a stress–strain curve, one can demonstrate nonlinearity and exclude a linear model, but that is insufficient to distinguish QLV from nonlinear superposition. To do that, one performs a series of relaxation studies at different strain or a series of creep studies at different stress. If the curves all have the same shape, then QLV is favored; if not, then a nonlinear superposition or a more general model (such as the Schapery model) is required. Recovery follows the same time dependence as relaxation or creep if the material is linearly viscoelastic or obeys nonlinear superposition. Study of the detailed time dependence of the recovery curves allows one to discriminate between nonlinear superposition and the Schapery model or other more general models [6] (see reference for more detailed discussion).

The primary goal, therefore, is to perform a series of experiments to determine the ability of nonlinear superposition, QLV and the Schapery nonlinear viscoelastic model to predict behavior of tendon and ligament. Secondary goals include comparing the viscoelastic behavior of tendon and ligament, using porcine digital flexor tendon and medial collateral ligaments as representative tissues, as well as comparing the Schapery model to other single integral models.

2. Methods

2.1. Specimen preparation

Eighteen digital flexor tendons and eighteen medial collateral ligaments were carefully excised from porcine legs for *ex vivo* testing. All extraneous tissue was removed with care not to disrupt insertion sites. Intact bone remained attached to the distal end of the flexor tendon, and both ends of the MCL remained attached to portions their respective bone. Specimens were kept hydrated in a physiologic buffered saline solution. Un-deformed area (a_0) was measured assuming an elliptical shape with long and short axis measurements taken at four points along the specimen with a digital caliper and averaged.

2.2. Mechanical testing

All mechanical testing was performed on a servohydraulic mechanical test system (Bionix 858; MTS, Minneapolis, MN, USA). Specimens were anchored in the machine by two grips, one each at the distal and proximal ends. The ligaments, having two bony ends, were secured in two stainless steel bone

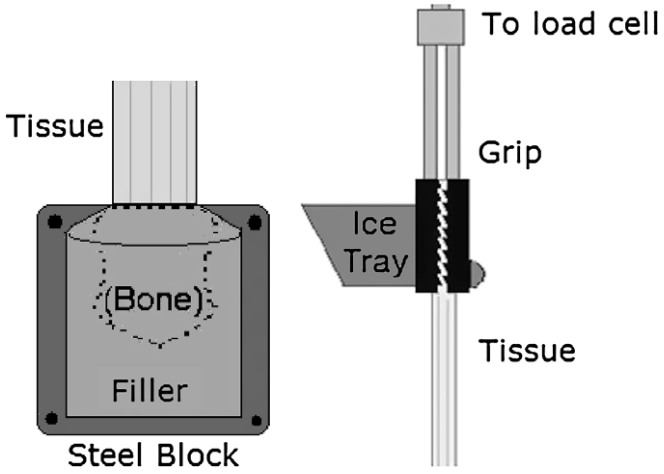

(a) (b)

Fig. 1. (a) Diagram of the "bone block" used to secure bony ends of specimens. The steel block contained two halves which could be securely screwed together to hold the bone (potted in filler shown) in place without risk of movement during testing. (b) Diagram of soft tissue grip used to secure the soft tissue end of tendon. The grip consisted of two plates having rough "saw-like" surfaces which gripped the tendon securely, and were screwed tightly together. Attached to the grip is a tray for holding dry ice during experiments to freeze the grip and prevent slip.

blocks (see Fig. 1a). The tendons, having one bony end and one soft tissue end, were secured using one bone block and a custom-made soft tissue grip (see Fig. 1b). Prior to testing, bony ends were embedded in polyester resin filler (with care taken to ensure tendon/ligament tissue and insertion sites were not encased in the filler) inside a mold matching the dimensions of the steel blocks to ensure a tight fit in the bone block with no slippage. Load was measured using a 50 lb load cell (Eaton Corporation) during testing, and grip-to-grip displacement was controlled by the servohydraulic test system. Once anchored in the machine, specimens were preloaded just to the point of loss of laxity (approximately 1 N for the tendon specimens, and 0.5 N for the ligament specimens). All mechanical testing occurred in a saline bath at ambient room temperature to maintain specimen hydration.

2.3. Preconditioning loop

Following preloading, all specimens were subjected to a preloading protocol which involved a sinusoidal wave to 2% strain (10 cycles in 20 s). This was followed by a step strain to 2%, which was held for 100 s and released. It was important to precondition all specimens as it has been reported in the literature that the first "preconditioning" stretch in a connective tissue results has slight irreversible effects [23,26]. The specimen was then allowed to rest for 1000 s prior to future testing protocols.

2.4. Relaxation rate comparison

In order to validate the claim that the rate of relaxation in tendon and ligament follow different trends, six digital flexor tendons and six MCL specimens were subjected to stress relaxation testing at various strain levels. Each specimen underwent stress relaxation testing for 100 s at 1–6% strain, in randomized order. The strain onset was treated as a step, with data collection beginning at $t = 2.5t_r$, where t_r is the rise time of the machine (in our case, $t_r = 0.04$ s). Justification for such design can be found in [7]. The level of strain, defined as the grip-to-grip displacement divided by the initial length of the specimen,

remained in the physiologically relevant range. Gardener et al. reported that the maximum strain in the human MCL during passive knee flexion was 5.8 ± 3.5% [12], and Lochner et al. reported that the maximum strain in equine flexor tendons during walking was in excess of 5% [18], so strain of 6% was chosen as the maximum physiological strain.

2.5. Three step protocol

Twelve tendon and twelve ligament specimens were subjected to a three step strain input protocol (see Fig. 2). The input followed a "hill-and-valley" pattern, with one low strain level sandwiched between two higher strains. This style of input allowed for a 100 s period of stress relaxation, followed by a 100 s period of recovery, followed by a second 100 s period of stress relaxation. Thus, not only was stress relaxation evaluated, but also the subsequent recovery (at a non-zero strain level so force data could be monitored), as well as the next stress relaxation. The second stress relaxation curve would display any ramifications of over- or under-predicting the recovery period of the pattern. In addition to allowing analysis of both relaxation and recovery, and simplifying the calculation of constitutive models, this pattern approximates the general strain pattern during running and walking, albeit at a much slower frequency. *In vivo* tendon and ligament loading during such activities involves rapid onset of load followed by a short time of sustained load, followed by rapid drop in load [16,18,22].

Two regions of strain were examined; a strain range near literature values of maximum *in vivo* strain was examined to ensure that results would be relevant to physiological models, and a low strain range was examined in order to observe the behavior of the tissues while still in the toe region, which is the strain range generally experienced by tendon and ligament during motion. One group of specimens,

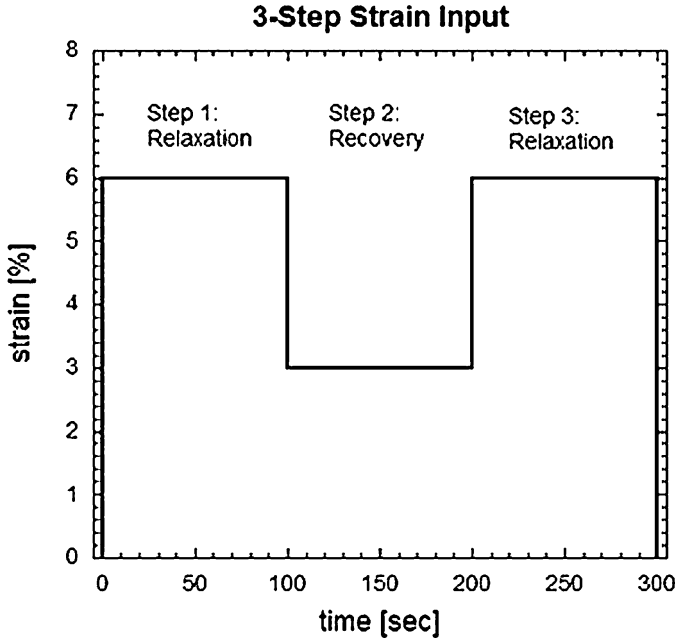

Fig. 2. Input strain wave to generate the 3-step model. "High physiologic" strain range testing is shown, with stress relaxation occurring at 6% strain (relative to preloaded state) and recovery at 3% strain. For "low physiologic" strain range testing, the same pattern occurs, with stress relaxation occurring at 2% strain (rather than 6%) and recovery occurring at 1% strain (rather than 3%).

comprised of six digital flexor tendons and six medial collateral ligaments, was subjected to the "high physiological" strain range. The second group of specimens, also containing six tendons and six ligaments, was subjected to the "low physiological" strain range, with maximal strain of 2%, in order to examine the low-strain behavior. In both groups, strain is defined as the grip-to-grip displacement divided by the initial length of the specimen.

Following the three step protocol testing, specimens were also subjected to two stress relaxation tests, one at the relaxation strain level (6% for high physiological strain, 2% for low physiological strain) and one at the recovery strain level (3% for high physiological strain, 1% for low physiological strain). Data from these relaxation curves would be used for model predictions (see Section 2.6).

2.6. Constitutive equations

The relaxation modulus was computed using the data from the 6% and 3% strain (2% and 1% strain for low range) relaxation experiments. The relaxation modulus is defined as

$$E(t, \varepsilon) = \sigma(\tau)/\varepsilon_0, \tag{1}$$

where ε_0 is the strain input and $\sigma(t)$ is the measured stress, calculated by

$$\sigma(t) = F(t)/a_0, \tag{2}$$

where $F(t)$ is the recorded force and a_0 is the undeformed area. The resulting curves for 6% and 3% (2% and 1%) strain were fitted with power law equations (of the form At^n), as these have been shown to fit data for tendon and ligament in the past [7,20].

The $E(t, \varepsilon)$ data collected from these curves was then used in the calculation of constitutive equations. The first constitutive model considered was nonlinear (modified) superposition [27], as it is relatively simple to calculate and has been shown to fit the stress relaxation of connective tissues well [7,20]. The general form of nonlinear superposition is given by

$$\sigma(\varepsilon, \tau) = \int E[t - \tau, \varepsilon(\tau)] \frac{\mathrm{d}\varepsilon(\tau)}{\mathrm{d}\tau}\, \mathrm{d}\tau. \tag{3}$$

A step strain input allows the equation to be simplified to

$$\sigma(t) = \varepsilon_a E(t, \varepsilon_a) - (\varepsilon_a - \varepsilon_b) E(t - t_1, \varepsilon_b), \tag{4}$$

where t is the time from the start of stress relaxation at the first step strain, and t_1 is the time at which recovery begins. Data from earlier performed relaxation curves ($E(t, \varepsilon)$) at 6% and 3% (2% and 1%) strain were used for calculation of the A and n parameters for the model.

The linear form of this superposition is given by the Boltzmann superposition integral:

$$\sigma(t) = \int E(t - \tau) \frac{\mathrm{d}\varepsilon(\tau)}{\mathrm{d}\tau}\, \mathrm{d}\tau, \tag{5}$$

in which E depends only on time, not strain. The use of a step strain input allows simplification of the equation to

$$\sigma(t) = \varepsilon_a E(t) - (\varepsilon_a - \varepsilon_b) E(t - t_1); \tag{6}$$

$E(t)$ is dependent only on time in linear viscoelasticity.

Another special case of nonlinear superposition in which the kernel, $E(t, \varepsilon)$ can be separated into the product of the time-dependent modulus, $E(t)$, and the strain-dependence, $g(\varepsilon)$, is quasi-linear viscoelasticity [10], generally described by

$$\sigma(t) = \int_0^t E_t(t-\tau)\frac{\mathrm{d}\sigma}{\mathrm{d}\varepsilon}\frac{\mathrm{d}\varepsilon(\tau)}{\mathrm{d}\tau}\,\mathrm{d}\tau. \tag{7}$$

This model has been frequently utilized in the literature to describe soft tissue behavior, despite the additional complexity involved. Use of a step strain input reduces the equation to

$$\sigma(t) = (\varepsilon_a)E_t(t)g(\varepsilon_a) - (\varepsilon_a - \varepsilon_b)E_t(t-t_1)g(\varepsilon_b). \tag{8}$$

Parameters for the model, including those for the reduced relaxation function g, were obtained by curve-fitting the data.

The $E(t, \varepsilon)$ data collected from these curves was also used to evaluate Schapery's model, which has been more frequently used to describe polymer behavior than biological phenomena. The general form of Schapery's model describing nonlinear stress relaxation is as follows:

$$\sigma(t) = h_e E_e + h_1 \int_{0-}^{t} \Delta E(\rho - \rho')\frac{\mathrm{d}h_2}{\mathrm{d}\tau}\,\mathrm{d}\tau, \tag{9}$$

where h_1, h_2 and h_e are strain-dependent properties related to Helmholtz free energy, E_e is the equilibrium modulus defined as $E_e = E(\infty)$, found by calculating $E(t)$ at the longest time point, ΔE is the transient modulus defined as $\Delta E = E(t) - E_e$, and ρ and ρ' (time variables, *not density*) are defined as

$$\rho \equiv \int_0^t \frac{\mathrm{d}t'}{a_\varepsilon}[\varepsilon(t')], \quad a_\varepsilon > 0, \tag{10}$$

$$\rho' \equiv \rho(\tau) = \int_0^\tau \frac{\mathrm{d}t'}{a_\varepsilon}[\varepsilon(t')], \tag{11}$$

where a_ε is a fourth strain-dependent property related to strain influences in entropy and free energy production, and ρ can be considered an "internal time" which can depend on strain [24]. Using a step strain input allows the integral equation to be further simplified to

$$\sigma(t) = \left[h_e^a E_e + h_1^a h_2^a \Delta E_a\left(\frac{t}{a_e^a}\right)\right]\varepsilon_a \tag{12}$$

for $0 < t < t_a$, and

$$\begin{aligned}\sigma(t) = &\left[h_e^b E_e + h_1^b h_2^b \Delta E_b\left(\frac{t-t_a}{a_\varepsilon^b}\right)\right]\varepsilon_b \\ &- \left(\frac{h_1^b}{h_1^a}\right)h_1^a h_2^a\left[\Delta E_a\left(\frac{t-t_a}{a_\varepsilon^b}\right) - \Delta E_a\left(\frac{t_a}{a_\varepsilon^a} + \frac{t-t_a}{a_\varepsilon^b}\right)\right]\varepsilon_a\end{aligned} \tag{13}$$

for $t_a < t < t_b$, where ε_a denotes the first strain level and ε_b denotes the second strain level, and $E_a(t)$ is shorthand for $E(t, \varepsilon_a)$.

Tendon and ligament are fibrous composites, so under isothermal conditions and uniaxial loading, it has been shown that $h_1 = a_\varepsilon = 1$ [24]. This simplifies the equation to

$$\sigma(t) = [h_e^a E_e + h_2^a E_a(t) - E_e]\varepsilon_a \tag{14}$$

for $0 < t < t_a$ and

$$\sigma(t) = [h_e^b E_e + h_2^b E_b(t - t_a) - E_e]\varepsilon_b - h_2^a[E_a(t - t_a) - E_a(t)]\varepsilon_a \tag{15}$$

for $t_a < t < t_b$. Parameters h_e and h_2 were obtained using fitting of experimental data in the same fashion as Provenzano et al. [21].

In order to evaluate the ability of the constitutive models to predict tendon and ligament behavior, stress was calculated from the force data (see Eq. (2)) acquired during the three step strain input (relaxation, recovery and second relaxation) and plotted with the models for comparison.

2.7. Statistical analysis

In order to assess the comparative ability of each of the constitutive models to fit and predict experimental data during the three step protocol, the root mean squared error (RMSE) was calculated. In this manner, it was possible to evaluate the deviation of each of the constitutive models from the experimental data in each step (relaxation, recovery and next relaxation). t-tests were performed with the Bonferroni correction applied on the resulting RMSE values in order to determine whether the RMSE of each model was significantly larger than any other model (p-values less than 0.05 were considered statistically different).

3. Results

3.1. Relaxation rate comparison

Figure 3 shows the results of stress relaxation experiments performed at various strain levels. Figure 3a is a plot of the stress relaxation of digital flexor tendon at various strains, and Fig. 3b contains the data from stress relaxation of the MCL at various strains. The trend in tendon (Fig. 3a) is that the rate of stress relaxation increases with increasing strain level, whereas the trend in ligament (Fig. 3b) shows that as strain level increases, the rate of stress relaxation decreases. This behavior is consistent with the nonlinear superposition and Schapery models, but not with QLV. The trends are further demonstrated in Fig. 4a and 4b, which plot the rate of relaxation as a function of strain for tendon (4a) and ligament (4b); the predictive lines of Schapery and nonlinear superposition are shown, as well as the flat-line prediction of QLV. This demonstrates the differing viscoelastic behavior of tendon and ligament, and the deviation from QLV.

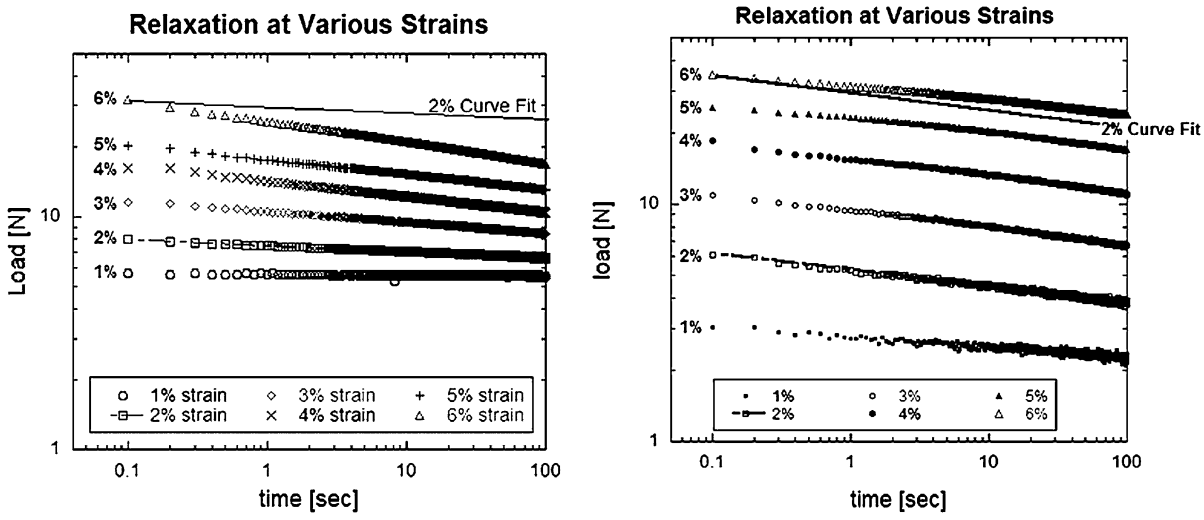

(a) (b)

Fig. 3. Stress relaxation at various strains. (a) Porcine digital flexor tendon results. QLV predicts all curves will have the same slope; experimental data show increasing slopes as strain level increases (highest at 6% strain, lowest at 1% strain). (b) Porcine MCL results. Notice the opposing trends: the rate of relaxation increases with increasing strain in flexor tendon, but decreases with increasing strain in MCL (highest at low strains, lowest at 6% strain). QLV predicts a uniform slope, which is not the case for either tissue.

3.2. Three step protocol

Figure 5 shows representative results of the three step input protocol for digital flexor tendon. Figure 5a is a plot of experimental data along with the constitutive models in the high physiological range, and Fig. 5b shows the results of the low physiologic strain testing. The general trend in both cases is that the initial stress relaxation (step one of the protocol) was fit well by the Schapery, QLV and nonlinear superposition models for a single test at one strain. The stress levels reached during the following recovery (step two) and second relaxation (step three) were better predicted by the Schapery model than nonlinear superposition and QLV models, though the initial shape of the recovery curve was not fit well by any model. Overall, the curve fits for the three step protocol are not as close as for a single step, because the models are required to fit a larger domain of behavior.

Figure 6 shows representative results of the three step input protocol for the medial collateral ligament. Figure 6a shows the experimental three step protocol data at high physiological strain, and Fig. 6b shows the results of low physiologic strain testing. In both strain cases, all three models fit the experimental data from the initial step for a single strain well, and subsequent loading steps are predicted well by Schapery model but overestimated by nonlinear superposition and QLV. Stress levels during recovery were better predicted by Schapery model, but again the initial shape of the recovery curve was not well fit by any model.

3.3. Statistical analysis

Calculated root mean squared error (RMSE) values for model fitting and predicting of the three steps are displayed in Table 1. RMSE values were not significantly different in the first step. In the second step, the RMSE values for the Schapery model were statistically smaller than those for both nonlinear

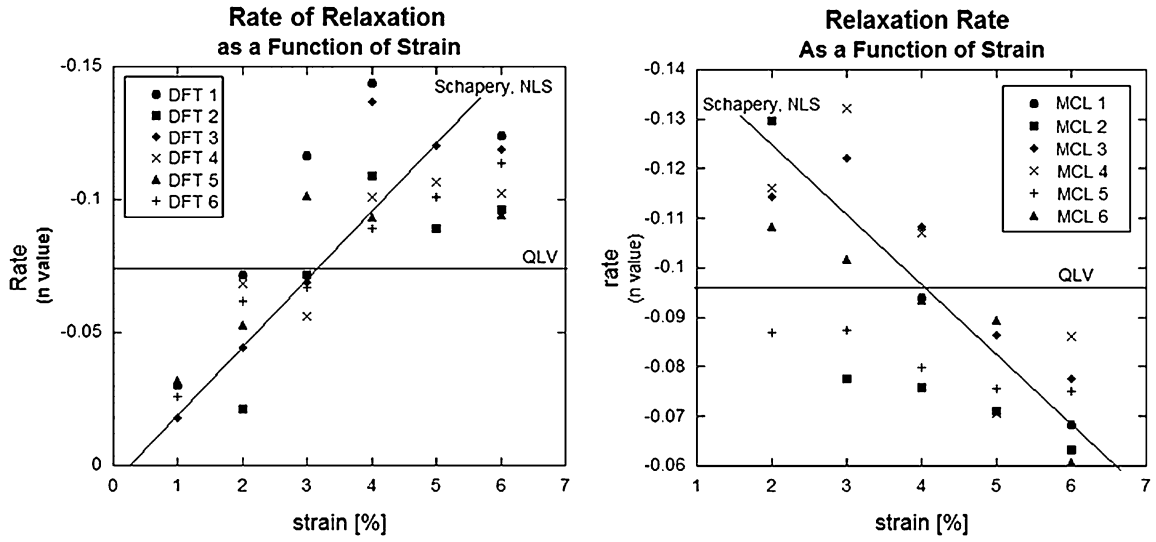

(a) (b)

Fig. 4. Graphs displaying rate of relaxation (defined as n term of power law equation, $E = At^n$) as a function of strain for (a) digital flexor tendon and (b) MCL. Notice the opposing trends: digital flexor tendon relaxation rate increases with increasing strain, while MCL relaxation rate decreases with increasing strain.

Table 1
Root mean squared error (RMSE) values of model fits for the three steps shown in Figs 5 and 6

		High		Low	
		DFT	MCL	DFT	MCL
Step 1	Schapery	0.30 ± 0.04	0.12 ± 0.11	0.010 ± 0.004	0.013 ± 0.006
	NLS	0.24 ± 0.11	0.15 ± 0.13	0.021 ± 0.013	0.021 ± 0.182
	QLV	0.24 ± 0.11	0.15 ± 0.13	0.021 ± 0.013	0.021 ± 0.182
Step 2	Schapery	$0.63 \pm 0.36^{*\prime}$	$0.07 \pm 0.03^{*\prime}$	$0.017 \pm 0.001^{*\prime}$	$0.001 \pm 0.004^{*\prime}$
	NLS	2.44 ± 0.33	0.32 ± 0.26	0.059 ± 0.049	0.078 ± 0.057
	QLV	2.53 ± 0.12	0.37 ± 0.24	0.076 ± 0.062	0.090 ± 0.047
Step 3	Schapery	$0.29 \pm 0.11^{*\prime}$	$0.02 \pm 0.01^{\prime}$	0.027 ± 0.033	$0.014 \pm 0.014^{\prime}$
	NLS	2.07 ± 0.57	0.24 ± 0.26	0.082 ± 0.069	0.050 ± 0.042
	QLV	2.20 ± 0.78	0.29 ± 0.24	0.064 ± 0.022	0.067 ± 0.030

Notes: $^{\prime}$RMSE value for Schapery significantly smaller than for quasi-linear viscoelasticity (QLV);
*RMSE value for Schapery significantly smaller than for nonlinear superposition (NLS).

superposition and QLV in all four cases (DFT and MCL undergoing high and low physiologic strain). In the third step, the RMSE values for the Schapery model were statistically smaller than those for QLV and nonlinear superposition in all cases except the DFT undergoing low physiologic strain.

4. Discussion

Results from the first step (initial relaxation) in both tendon and ligament, as well as in both the high physiological strain and low physiological strain ranges, show that all three single integral models fit the

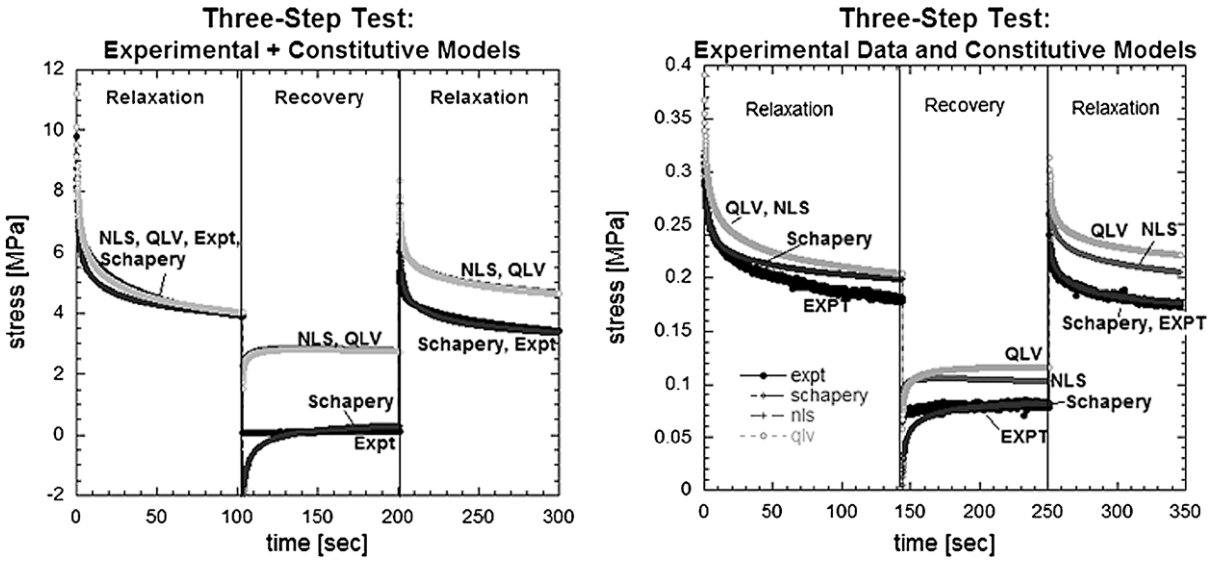

(a) (b)

Fig. 5. Experimental data from three step testing of porcine digital flexor tendon fitted with the Schapery model (see Eq. (6)), nonlinear superposition model (see Eq. (8)), and QLV (see Eq. (10)). Models are generated by fitting of the three steps (see Sections 2.5 and 2.6). (a) High physiologic strain levels (step one: relaxation at 6% strain for 100 s, step two: recovery at 3% strain for 100 s, step three: relaxation at 6% strain for 100 s). All models fit the initial stress relaxation curve (at a single strain), but nonlinear superposition and QLV models over-predict recovery following relaxation, as well as the following relaxation curve. The Schapery model predicts compressive loads when strain is reduced from 6% to 3%, which does not occur in soft tissue such as tendon and ligament (which go slack rather than undergoing compression in this setup). (b) Low physiologic strain testing (step one: relaxation at 2% strain 100 s, step two: recovery at 1% strain 100 s, step three: relaxation at 2% strain 100 s). The Schapery model provides a good fit of the experimental data in recovery and subsequent loading.

stress relaxation curve of the experimental data of both strain cases (high and low) and both tissue types (tendon and ligament) well at one strain. If multiple strain levels are applied in subsequent relaxation experiments, however, the relaxation rate depends on strain (the rate of relaxation in the tendon increases as strain increases, while in the ligament it decreases as strain increases). This behavior is successfully modeled by nonlinear superposition and by Schapery, but not by QLV.

The second step, the recovery portion, shows more interesting behavior. In both physiological and low strain cases, as well as in both the tendon and ligament, the recovery progresses at a slower rate (with rate defined as the exponent n in the power law equation) than stress relaxation. This may be in part due to asymmetrical biomechanical behavior resulting from differences in loading and unloading conditions (loading occurs via a forced displacement, while recovery loads result from internal processes in the unloaded state). If such asymmetry exists, it would complicate a symmetrical model's ability to predict both relaxation and recovery, requiring a more advanced model to fit the shape accurately. When looking at the physiological strain range, it is evident that in both the medial collateral ligament and the digital flexor tendon the nonlinear superposition and quasi-linear viscoelasticity (QLV) over-predict stress during recovery. The Schapery model, on the other hand, provides a much better fit of recovery stress level, with a significantly lower root mean squared error. The main caveat to this model is the prediction of compression during the step strain reduction, marked by a large jump in stress in the negative direction and a more gradual increase (as opposed to the quick increase seen in the experimental behavior). Compression such as this would exist if the material was rigid, but both tendon and ligament are soft tissues, and they will collapse to a slack state rather than generate compressive loads. After a few

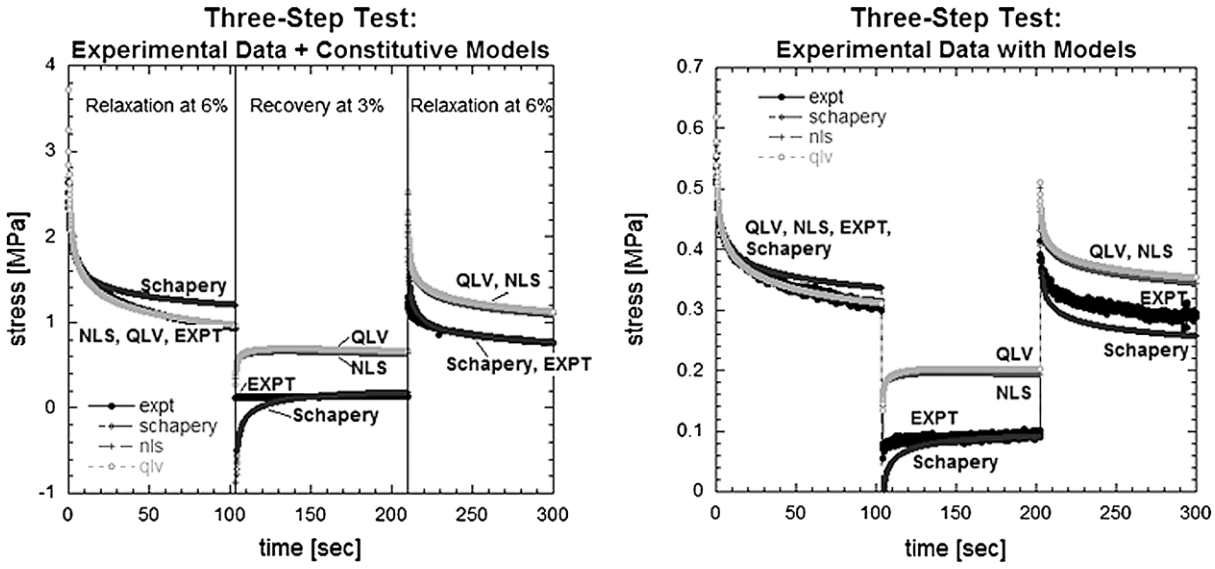

Fig. 6. Experimental data (EXPT) from three step testing of MCL fitted with QLV, nonlinear superposition (NLS), and Schapery's nonlinear viscoelastic models, which are generated by fitting of the three steps (see Sections 2.5 and 2.6). (a) High physiologic strain (step one: relaxation at 6% strain, step two: recovery at 3% strain, step three: relaxation at 6% strain). (b) Low physiologic strain (step one: relaxation at 2% strain, step two: recovery at 1% strain, step three: relaxation at 2% strain). The Schapery model provides a good fit of all three steps in each strain case; QLV and nonlinear superposition fit the first relaxation but over-predict the stress levels of the next two steps.

seconds, the compression stress is no longer a factor, and the Schapery model predicts the recovery of the tendon and ligament quite well. The RMSE values for the QLV and nonlinear superposition models were roughly 4 times that of the Schapery model for tendon at high and low strains and ligament at high strains, and more than 10 times larger for the ligament tested at low strain.

The third step, a second relaxation, displays the consequences of incorrectly predicting the second step. Both the nonlinear superposition and the QLV model over-predict the stress reached during the second relaxation in both tendon and ligament specimens. The Schapery model, which provided a more accurate prediction of stress levels in the second step, also provided a more accurate prediction of the second relaxation. The RMSE values for QLV and nonlinear superposition in this step was over 7 times larger than the RMSE for Schapery in the high strain tendon testing, and in the high strain ligament testing the RMSE values for QLV and nonlinear superposition were 12 and 14.5 times greater, respectively, than that for the Schapery model. The data from this step, along with the previous two, indicate that while all three models are capable of data-fitting, the Schapery model is robust enough to predict further behavior.

The ability of the Schapery model to fit both of these tissues is impressive as the porcine MCL and digital flexor tendon display differing viscoelastic behavior under the same testing conditions. By performing stress relaxation experiments at different strains, it was possible to observe the relative rates of relaxation at various strain levels in tendon and ligament, and compare the trends. For the case of the digital flexor tendon, the rate of relaxation is greatest at higher strains and decreases with decreasing strain. The opposite is true of the MCL, for which the rate of relaxation is greatest at lowest strains and decreases with increasing strain. Interestingly, the rate of relaxation in the porcine MCL appears less strain dependent than porcine flexor tendon or previously reported data on rat MCL [21]. Thus it

appears that the strain dependence of the relaxation rate is variable between species, as well as between tissues in the same species.

The constitutive models evaluated in this study were chosen because they were all single integral models, and therefore relatively easy to calculate, especially in step loading inputs frequently used in stress relaxation and creep testing. The nonlinear superposition model is the simplest of the three models; it can be constructed by calculating $E(t, \varepsilon)$ from the data (see Eq. (1)) and substituting them in Eq. (3) and/or (4). In our case, $E(t, \varepsilon)$ is assumed to follow power law behavior in time, of the form At^n. As such, it requires the fitting of the A and n parameters, each of which is dependent on strain. The construction of the QLV model entails calculation of both the elastic component and the reduced relaxation function. The elastic component, commonly described by the exponential expression $M(\mathrm{e}^{B\varepsilon} - 1)$, requires parameters M and B. Three additional parameters must be found in order to calculate the suggested reduced relaxation function $(g) : C, \tau_1$ and τ_2 [10,28]. The intensive calculations involved in the reduced relaxation function and the additional parameters make the QLV model more complicated, and the assumptions (strain rate insensitivity, and relaxation rate independence from strain level) make it less applicable to tendon and ligament. The Schapery model requires calculation of $E(t, \varepsilon)$ similar to nonlinear superposition, necessitating the fitting of A and n parameters, as well as thermodynamic parameters h_2 and h_e, in its construction [5,20,24]. The Schapery model is thus more complicated than the simple nonlinear superposition, with a total of four parameters, but without the complex relaxation function calculation, it is less complicated to calculate than QLV. Therefore, while QLV is more commonly used to describe soft tissue behavior, the Schapery model appears capable of describing the behavior of tendon and ligament even more robustly without creating additional model complexity.

Knowing the exact range of physiologic strain is difficult, as strain measurements are highly dependent on the definition of the "zero state" (length at which displacement is zero). Reported *in vivo* strain measurements vary considerably; Gardener et al. and Lochner et al. found the maximum *in vivo* strains in ligament and tendon to be 5–6% [12,18], while Haut noted that ligament strain during normal bodily activity is below 4% [14] and Fleming et al. found that ligament strain is typically 3.6% during squatting and 1.7% during biking [9]. *In vitro* strain measurements are dependent on the method of acquisition; strain measured optically is typically around 50–60% of the grip-to-grip strain recorded by the MTS system (unpublished results). While these variations make it difficult to pinpoint an exact strain range of interest, a robust model is predictive through a variety of strains. In this study, the Schapery model was able to predict the viscoelastic behavior of tendon and ligament at both the high and low strain ranges reported in literature. The robust nature of this model allows it to be predictive over the entire range of strains of interest in physiologic studies.

In summary, the nonlinear viscoelastic Schapery model successfully described the behavior of two connective tissues in single stress relaxation curves and a more complex loading protocol. QLV was able to fit a single stress relaxation curve, but did not describe the strain-dependent behavior of digital flexor tendon or MCL observed in this study, or accurately predict stress levels during recovery and subsequent loading. Nonlinear superposition accounted for the strain-dependent nature of tendon and ligament, but failed to accurately predict stresses reached during recovery and subsequent loading. The flexibility of the Schapery model allowed it to fit the differing viscoelastic behaviors of porcine digital flexor tendon and porcine MCL, and it was much more successful at predicting stresses reached during recovery and future loading. Thus, it follows that the Schapery model is the most robust of the constitutive equations examined here in the physiological strain range examined. It has the potential to improve on biomechanical modeling of joint kinematics, particularly when considering complex or cyclic loadings.

Acknowledgements

This work was funded by NSF award 0553016. The authors thank Ron McCabe for his technical assistance.

References

[1] S.D. Abramowitch and S.L.-Y. Woo, An improved method to analyze the stress relaxation of ligaments following a finite ramp time based on the quasi-linear viscoelastic theory, *J. Biomech. Eng.* **126** (2004), 92–97.
[2] P.J. Arnoux, P. Chabrand, M. Jean and J. Bonnoit, A visco-hyperelastic model with damage for the knee ligaments under dynamic constraints, *Computer Meth. Biomech. Biomed. Eng.* **5** (2002), 167–174.
[3] C. Bonifasi-Lista, S.P. Lake, M.S. Small and J.A. Weiss, Viscoelastic properties of the human medial collateral ligament under longitudinal, transverse, and shear loading, *J. Orthop. Res.* **23** (2005), 67–76.
[4] P. Ciarletta, S. Micera, D. Accoto and P. Dario, A novel microstructural approach in tendon viscoelastic modeling at the fibrillar level, *J. Biomech.* **39** (2006), 2034–2042.
[5] D.A. Dillard, M.R. Straight and H.F. Brinson, The nonlinear viscoelastic characterization of graphite/epoxy composites, *Polymer Eng. Sci.* **27** (1987), 116–123.
[6] S.E. Duenwald, R. Vanderby Jr. and R.S. Lakes, Constitutive equations for ligament and other soft tissue: evaluation by experiment, *Acta Mechanica* **205** (2009), 23–33.
[7] S.E. Duenwald, R. Vanderby Jr. and R.S. Lakes, Viscoelastic relaxation and recovery of tendon, *Ann. Biomed. Eng.* **37**(6) (2009), 1131–1140.
[8] D.M. Elliot, P.S. Robinson, J.A. Gimbel et al., Effect of altered matrix proteins on quasilinear viscoelastic properties in transgenic mouse tail tendons, *Ann. Biomed. Eng.* **31** (2003), 599–605.
[9] B.C. Fleming, B.D. Beynonon, P. Renstrom et al., The strain behavior of the anterior cruciate ligament during bicycling, an *in vivo* study, *Am. J. Sports Med.* **26** (1998), 109–118.
[10] Y.C. Fung, Stress–strain history relations of soft tissues in simple elongation, in: *Biomechanics: Its Foundations and Objectives,* Y.C. Fung, N. Perrone and M. Anliker, eds, Englewood Cliffs, Prentice Hall, NJ, 1972, pp. 181–208.
[11] J.R. Funk, G.W. Hall, J.R. Crandall and W.D. Pilkey, Linear and quasi-linear viscoelastic characterization of ankle ligaments, *J. Biomech. Eng.* **122** (2000), 15–22.
[12] J.C. Gardener, J.A. Weiss and T.D. Rosenberg, Strain in the human medial collateral ligament during valgus loading of the knee, *Clin. Orthop. Relat. Res.* **391** (2001), 266–274.
[13] J.A. Gimbel, J.J. Sarver and L.J. Soslowsky, The effect of overshooting the target strain on estimating viscoelastic properties from stress relaxation experiments, *J. Biomech. Eng.* **126** (2004), 844–848.
[14] R.C. Haut, The mechanical and viscoelastic properties of the anterior cruciate ligament and of ACL fascicles, in: *The Anterior Cruciate Ligaments, Current and Future Concepts*, D.W. Jackson, ed., Raven Press, New York, 1993, pp. 63–76.
[15] R.V. Hingorani, P.P. Provenzano, R.S. Lakes et al., Nonlinear viscoelasticity in rabbit medical collateral ligament, *Ann. Biomed. Eng.* **32** (2004), 306–312.
[16] D.L. Korvick, J.F. Cummings, E.S. Grood et al., The use of implantable force transducer to measure patellar tendon forces in goats, *J. Biomech.* **29** (1996), 557–561.
[17] J.S.Y. Lai and W.N. Findley, A modified superposition principle applied to creep of nonlinear viscoelastic material under abrupt changes in state of combined stress, *Trans. Soc. Rheol.* **11** (1967), 361–380.
[18] F.K. Lochner, D.W. Milne, E.J. Mills and J.J. Groom, *In vivo* and *in vitro* measurement of tendon strain in the horse, *Am. J. Vet. Res.* **41** (1980), 1929–1937.
[19] R.J. Minns, P.D. Soden and D.S. Jackson, The role of the fibrous components and ground substance in the mechanical properties of biological tissues: a preliminary investigation, *J. Biomech.* **6** (1973), 153–165.
[20] P.P. Provenzano, R.S. Lakes, D.T. Corr and R. Vanderby Jr., Application of nonlinear viscoelastic models to describe ligament behavior, *Biomech. Model Mechanobiol.* **1** (2002), 45–57.
[21] P. Provenzano, R. Lakes, T. Keenan and R. Vanderby, Nonlinear ligament viscoelasticity, *Ann. Biomed. Eng.* **29** (2001), 908–914.
[22] D.J. Riemersma, H.C. Schamhardt, W. Hartman and J.L.M.A. Lammertink, Kinetics and kinematics of the equine hind limb: *in vivo* tendon loads and force plate measurements in ponies, *Am. J. Vet. Res.* **49** (1988), 1344–1352.
[23] B.J. Rigby, N. Hirai, J.D. Spikes and H. Eyring, The mechanical properties of rat tail tendon, *J. Gen. Physiol.* **43** (1999), 265–283.
[24] R.A. Schapery, On the characterization of nonlinear viscoelastic materials, *Polymer Eng. Sci.* **9** (1969), 295–310.
[25] J. Sorvari, M. Malinen and J. Hämäläinen, Finite ramp time correction method for non-linear viscoelastic material model, *Int. J. Non-Linear Mech.* **41** (2006), 1050–1056.

[26] A. Sverdlik and Y. Lanir, Time-dependent mechanical behavior of sheep digital tendons, including the effects of preconditioning, *J. Biomech. Eng.* **125** (2002), 78–84.
[27] I.M. Ward and E.T. Onat, Non-linear mechanical behaviour of oriented polypropylene, *J. Mech. Phys. Solids* **11** (1963), 217–229.
[28] S.L. Woo, M.A. Gomez and W.H. Akeson, The time and history-dependent viscoelastic properties of the canine medial collateral ligament, *J. Biomech. Eng.* **103** (1981), 293–298.